A benchmark estimate of the effect of anthropogenic emissions on the ocean surface

Dáithí A. Stone[1] and Pardeep Pall[1]

[1]Lawrence Berkeley National Laboratory,

Berkeley, California, U.S.A.

Abstract.

Investigations into the role of anthropogenic emissions in the occurrence of extreme weather often use a method that compares simulations of atmospheric climate models under factual conditions that have been experienced against simulations under counterfactual conditions that might have been experienced at that time in the absence of emissions. The particular challenge for this experimental design is the estimation of ocean surface boundary conditions for use by the counterfactual simulations. So far, studies have usually used a single bespoke estimate, leading to difficulty in understanding the nature of uncertainties in results. Here we develop an estimate of sea surface temperatures and sea ice conditions for use in counterfactual simulations, intended as a benchmark estimate to facilitate comparison across climate models and across studies. This development includes tests to ensure that the final estimate is stable from year-to-year and stable against other perturbations to the methodology. While the estimate is tailored specifically for the International CLIVAR C20C+ Detection and Attribution Project, it should be relevant for use by related projects as well.

1. Introduction

Growing interest in the role of anthropogenic emissions in recent and current extreme weather has been reflected in a rapidly growing number of studies [*Stott et al.*, 2013; *Bindoff et al.*, 2013; *Herring et al.*, 2014]. Despite the growth, this field of research remains ad hoc, with no climate model-based products optimised for general application. For instance, standard climate model databases, such as the CMIP5 archive [*Taylor et al.*, 2012], have at most a handful of simulations per climate model driven under the historical forcing scenarios required for attribution analysis, providing small sample sizes for the analysis of extreme weather. To address this gap a number of institutions around the world are collaborating on the Climate of the 20th Century Plus (C20C+) Detection and Attribution (D&A) Project with a primary goal of generating a new data product optimised for understanding extreme weather under anthropogenic climate change [*Folland et al.*, 2014].

The C20C+ D&A Project adopts the time-slice experimental design first introduced by *Pall et al.* [2011]. This involves generating large ($\geq$50 member) ensembles of simulations, each with a different initial state, with an atmospheric model driven under two scenarios: a factual scenario (denoted "All-Hist" in the C20C+ D&A Project) representing the boundary conditions experienced over the past several decades; and a counterfactual scenario ("Nat-Hist") representing a natural world that might have been had human activities not interfered with the climate system. The design will permit comparisons of trends in the All-Hist simulations against observed trends, diagnosis of patterns of large scale circulation related to extreme weather in the All-Hist simulations, or comparison of the All-Hist versus Nat-Hist simulations. This experimental design has the advantage of allowing the generation of very large (i.e. $\geq$50 member) ensembles of simulations with climate models at relatively high spatial resolution, because the "spin-up" time scale required for the atmospheric models is much shorter than what is required for models of the full climate system. The trade-off is that short time-scale coupling between the ocean surface and the atmosphere is lost, which can limit the type of events that can be examined with this approach [*Trenberth et al.*, 2015], and variations in ocean conditions are limited to those that actually occurred, rather those that are potentially realisable under past and current boundary conditions, which limits the generality of results.

Under both scenarios, simulations are driven by time-varying boundary conditions (Table 1). For the All-Hist scenario, these comprise greenhouse gas concentrations, tropospheric aerosol burdens (or emissions), stratospheric (volcanic) aerosol burdens (or emissions), ozone concentrations, land cover, solar luminosity, sea surface temperatures, and sea ice concentrations. For the Nat-Hist scenario, though, greenhouse gases, anthropogenic aerosols, and ozone conditions are set to pre-industrial values, and the ocean surface conditions are adjusted accordingly. The specification of these boundary conditions follows easily from current practice [e.g. *Taylor et al.*, 2012] or from the experimental design, except for the specification of the Nat-Hist ocean surface conditions. The only studies to start exploring sensitivity to this uncertainty have found notable differences in event attribution results between these samples [*Pall et al.*, 2011; *Kay et al.*, 2011; *Christidis et al.*, 2013; *Christidis and Stott*, 2014].

This paper focuses on developing a benchmark estimate, dubbed "Nat-Hist/CMIP5-est1", of the Nat-Hist sea surface temperatures (Section 3) and sea ice concentrations

(Section 4) for use by the C20C+ D&A Project and, hopefully, by other projects. The intention is not that this should be the only estimate used: indeed, contributors to the C20C+ D&A Project are encouraged to produce Nat-Hist ensembles for at least three different attributable ocean warming estimates. Rather, the intention is to produce a plausible estimate that can be used for intermodel comparison studies. As such, it is recommended as the first attributable warming estimate to be used by contributors to the C20C+ D&A Project, as well as an option for other projects that would facilitate cross-project comparison.

2. Data

2.1. Selection of data

The All-Hist scenario uses observed ocean surface conditions, so to allow a comparison of "like against like" between the two scenarios it is necessary to preserve the anomalous month-to-month and year-to-year variability of the observed conditions. A solution is to subtract an attributable warming estimate from the observed conditions, where this estimate describes the spatially and seasonally varying warming response to anthropogenic emissions. Crucially, it varies only slowly in time, consistent with the gradual influence of anthropogenic emissions (any nonlinear influence of volcanic eruptions will be examined below).

The attributable warming estimate is intended to be a benchmark for widespread use, and thus not only must it be a physically plausible estimate, but it must also be derived from data sources and with methods that are widespread, preferably without being overly complicated. In order to be appropriate for widespread application, its stability to perturbations to various aspects of its generation also needs to be understood. A number of plausible estimates exist already. Estimates based on simulations of a single atmosphere-ocean climate model have been produced and used [*Pall et al.*, 2011; *Christidis et al.*, 2013; *Shiogama et al.*, 2013; *Christidis and Stott*, 2014; *Wolski et al.*, 2014], but as candidates for benchmarks we consider them to have two important issues: the selection of the climate model is arbitrary; and their robustness has yet to be examined in detail. *Christidis and Stott* [2014] propose instead using a map of observed linear trends in the historical record, which satisfies the simplicity requirement, but the pattern depends strongly on the interpolation method used to estimate temperatures over large areas of the ocean that were largely unmonitored a century ago [*Deser et al.*, 2010; *Hartmann et al.*, 2013; *Kennedy*, 2014]; *Bichet et al.* [2015], instead using pattern scaling methods, conclude that at most half of the resulting pattern reflects a response to anthropogenic forcing. These options all represent plausible estimates of the anthropogenic ocean warming response. However, because we feel these options do not satisfy all of the above criteria for a widely-used benchmark, we develop an alternative here that we argue satisfactorily fits the purpose.

The "historical" (representing historical changes in climate driven by both anthropogenic and natural forcings) and "historicalNat" (driven by natural forcings only) simulations from the CMIP5 climate model database [*Taylor et al.*, 2012] have become the international standard for estimating how we expect the average climate to have evolved over the past century (historical) and how we expect it might have evolved in the absence of anthropogenic interference (historicalNat) [*Bindoff et al.*, 2013]. These simulations have been generated using state-of-the-art coupled atmosphere-ocean models of the climate system and thus are intended to account for all possible sources of climate variability on time scales ranging up to the full one and a half centuries covered. Thus we adopt these simulations for estimation of the Nat-Hist benchmark — dubbed "Nat-Hist/CMIP5-est1" — by taking the time-varying difference between the historical and historicalNat simulations. The CMIP5 historical simulations start before the beginning of the 20th century but end in the year 2005, so we extend them to (and beyond) the present using CMIP5 simulations driven with the RCP4.5 emissions scenario ("rcp45") which continue on from the end of the historical simulations. No such continuation exists for historicalNat simulations (some of which end later than 2005) so whenever a historicalNat simulation ends we adopt the final available year for use in subsequent years (the assumption of constant natural forcings underlies the RCP4.5 scenario as well).

The simulations used are listed in Table 2. Selection was based on:

- Availability on 1 April 2013.
- Availability of monthly skin temperature data from simulations following the historical, rcp45, and historicalNat scenarios.

By selecting historical and historicalNat simulations which share initial conditions, we assume that long-term secular drift is cancelled through the subtraction of the latter from the former. All data are regridded to the $1^\circ \times 1^\circ$ grid of the NOAA OI.v2 observational sea surface temperature and sea ice coverage product [*Reynolds et al.*, 2002], with data retained over ocean as well as over land.

2.2. Averaging across simulations

Either models or simulations could be treated as the basic unit for averaging. When considering differences between all-forcings and natural-forcings simulations over the recent past and near future, as here, natural autonomous variability of the climate system accounts for a large fraction of the spread of trends across simulations, which means that it is a common practice to consider each simulation as equally probable [e.g. *Hegerl et al.*, 2007; *Hoegh-Guldberg et al.*, 2014]. Our estimate follows this practice, which also provides a higher effective sample size that proves useful for reducing sampling "noise" at small scales (see Section 3.2). Taking only one simulation per model yields a similar difference map at large scales, but with some regional differences which could be relevant when simulating local or regional extreme weather (Figure 1); a large part of this difference is likely sampling noise in the smaller data set.

3. Attributable sea surface warming

3.1. Selection of skin temperature

The most obvious temperature measure to use for estimating changes in sea surface temperature might be sea surface temperature itself. However, because sea surface temperature cannot go below the freezing point, it cannot be used in the polar regions. *Pall et al.* [2011] used 1.5m near-surface temperature partly for this reason. Here though we opt for skin temperature. It more closely matches sea surface temperature in the ice-free open ocean, and over ice-covered regions it reports the temperature at the ice-air interface which corresponds to the surface boundary for atmospheric models.

3.2. Stability from year to year

Despite the use of 51 simulations for each of the historical+rcp45 and historicalNat scenarios, there may still be noticeable sampling "noise" at the grid scale of the attributable warming estimates, which could be important for simulation of regional extreme weather. Anthropogenic forcing is changing only slightly from year to year, so comparison of nearby years should reveal little difference if sampling noise is minimal. Figure 2 compares the attributable warming estimate for January 2006 against the estimate for January 2001 and reveals that, despite use of a large number of simulations, regional year-to-year variations as large as 0.5°C arise. One option would be to impose some spatial smoothing [*Shiogama et al.*, 2013], but this could remove local warming gradients that are important for the generation of extreme weather on and near coasts. Another option is to smooth in time [*Shiogama et al.*, 2013]. Use of a 5-year boxcar filter (note that still no data is shared for 2001 and 2006 calculations) applied separately for each calendar month reduces those variations to about 0.1°C (in ice-free areas) of the global average warming. Note that the large differences bewteen the maps in some areas in the interior of the continents should be irrelevant for prescribing ocean surface conditions.

One potential issue with a temporal filter is that it smooths out the climate response to volcanic eruptions. If the sea surface temperature response to a major volcanic eruption is linearly additive with the response to anthropogenic forcing [*Meehl et al.*, 2003; *Gillett et al.*, 2004; *Shiogama et al.*, 2012], then this issue will be resolved by the cancelation of volcanic responses in the calculation of the difference between the historical and historicalNat simulations. Figure 3 shows the difference in attributable ocean warming estimates for January 1992 (soon after the major eruption of Mt. Pinatubo) and for January 1997 (a while after, with no major eruptions occurring in the interim); no temporal smoothing was used for this map. The magnitude of the variations from a global average warming are comparable to those seen in Figure 2 for an eruptionless five-year interval when no temporal smoothing is applied. More systematically, the root-mean-squared differences between the spatial patterns of estimated attributable warming over the ocean for each calendar month (not shown) do not indicate anything special about the years during and following the major Mt. Agung, El Chichón, or Mt. Pinatubo eruptions. We therefore adopt the 5-year boxcar smoothing in all further calculations.

3.3. Amplitude of response

Is the estimated attributable warming plausible? We can evaluate the magnitude of the response through regression against the observed record. We take the global mean sea surface temperatures (skin temperature over water) averaged across all of the historical CMIP5 simulations listed in Table 2, do the same for the historicalNat simulations, and take the global mean from the *Hurrell et al.* [2008] observational product of sea surface temperatures. We then regress 5-year-averages of the historical and historicalNat signals using the total least squares regression approach [*Allen and Stott*, 2003, code at http://www.csag.uct.ac.za/∼daithi/idl_lib/detect], with the residual compared against available skin temperature data from unforced (i.e. no changes in external boundary conditions beyond the diurnal and annual cycles) "piControl" simulations from all of the CMIP5 models listed in Table 2 (except no data is available for BCC-CSM-1). The most likely estimate for the regression coefficient for the response to anthropogenic forcing is listed in Table 3 for a number of periods, domains, and months of the year.

For the century-long time scale, the most likely estimates for the regression coefficients are near 1, meaning that the magnitude of the Nat-Hist/CMIP5-est1 changes closely match the observed changes. However, the residual of the regression is significantly larger than would be expected with an adequate fit. This inconsistency results from an apparent warm bias in the CMIP5 models relative to observed values at the beginning of the 20th Century and an apparent cold bias in the middle of the century [*Ribes and Terray*, 2013]. This discrepancy can be at least partially reduced by accepting that the relative bias in the magnitude of the models' responses may differ for greenhouse gas forcing and anthropogenic aerosols forcing, i.e. through a regression analysis that isolates these responses [*Ribes and Terray*, 2013].

Perhaps a more relevant analysis, however, would examine the 1961–2010 period, both because the observational monitoring is more comprehensive for this period and because it more closely matches with periods likely to be examined in the C20C+ D&A Project and similar investigations. Because the temporal profile of the aerosol and greenhouse gas responses is similar (but opposite) over the past half century, an anthropogenic-natural regression analysis for the past half-century is able to produce an adequate fit to the observed record over this period, but at the cost of regression coefficients that are barely consistent with 1 (Table 3). This reflects that a 0.14°C cooling (over the 50°S–50°N ocean surface) over the 1961–2010 period arises when the unadjusted Nat-Hist/CMIP5-est1 attributable warming estimate is subtracted from the *Hurrell et al.* [2008] observational sea surface temperature product (which has a 0.48°C warming), and a 0.15° cooling when subtracted from the HadISST1 product [*Rayner et al.*, 2003]. This compares against an average 0.10°C warming in the CMIP5 historicalNat simulations. Thus, it may be possible to improve the accuracy of the Nat-Hist/CMIP5-est1 estimate of attributable ocean warming through adjustments based on a multi-signal regression analysis. However, we also note that the most recently published estimate of the observed rate of warming over the 1951–2012 period implies ~0.06°C more warming over the 1961–2010 period compared to the ocean temperature products considered above [*Karl et al.*, 2015]. In light of this uncertainty, the Nat-Hist/CMIP5-est1 estimate appears to have an acceptable possible warm bias and that the added complexity of a regression-based adjustment is not required. To allow sensitivity tests, though, we have also published a "Nat-Hist/CMIP5-est1-p50" estimate of natural ocean temperatures and sea ice coverage, by adjusting the amplitude of the attributable anthropogenic warming estimate by the 50th percentile of the probability distribution in the regression analysis for annual values over 1961–2010 spanning the 50°S–50°N ocean (0.83).

4. Sea ice coverage

Unfortunately, the attributable change in sea ice coverage cannot be detected in the same manner as the attributable ocean warming. Regional biases in sea ice extent in the CMIP5 models [*Mahlstein et al.*, 2013; *Flato et al.*, 2013; *Notz*, 2014], as well as inconsistencies in subtracting a mean difference from a temporally-varying observed extent, lead to implausible Nat-Hist estimates. Recognising this, *Pall et al.* [2011] instead developed an approach to alter sea ice coverage in a manner that is consistent with the estimated attributable warming in sea surface temperatures. This method involves determining a simple functional form to the temperature/ice-coverage relationship and modifying All-Hist ice coverage using this function. *Pall et al.* [2011] adopted a function, based on near-surface air temperature in a given reference observational data set, that depends on a linear fit passing through the freezing-point/full-coverage point and the median temperature/coverage point of all intermediate-coverage areas as determined from grid-cell-resolution data, which was estimated separately for each hemisphere. The function then followed three basic steps:

- If the Nat-Hist temperature is below the freezing point, enforce full coverage.
- While at temperatures above the intercept of the linear fit and no-coverage, maintain the All-Hist coverage.

• While the temperature is between the freezing point and the intercept of the linear fit and no-coverage, increase the coverage at the rate indicated by the linear fit.

The approach has been used by a number of recent studies [*Christidis et al.*, 2013; *Shiogama et al.*, 2013; *Christidis and Stott*, 2014], but its robustness against perturbations to the methodology have yet to be examined in detail. We adopt a similar function here except that the intermediate-coverage section is estimated using a bin-based approach. We calculate the median temperature in each of 100 equally-sized ice-coverage bins, and the new function is the line that connects the freezing-point/full-coverage point and the centre of mass of all of the bin medians. The calculations are performed on observed temperature/ice-coverage data over the 2001-2010 period using the NOAA OI.v2 observationally-based dataset [*Reynolds et al.*, 2002]. The result ends up being similar to the linear fit of *Pall et al.* [2011] (dashed red versus dashed blue lines in the plots in the top two rows of Figure 5). This bin-based empirical fit has a slope of m_d and a no-coverage intercept at SST_{open}, and is estimated and applied separately for the Northern and Southern Hemispheres and for each calendar month.

Given this function, the algorithm for determining the Nat-Hist ice coverage follows a series of steps, listed in Figure 4. The resulting changes are illustrated by the arrows in the top and middle right panels of Figure 5, when the Nat-Hist/CMIP5-est1 attributable warming estimate is applied to the NOAA OI.v2 observational product. A notable issue is that the function is limited in its ability to handle attributable coolling (i.e. sea ice retreat due to the Nat-Hist conditions being warmer than the observed/All-Hist conditions). In particular, because available observational products fix surface temperature to the freezing point when ice coverage is full, it is not possible to thin the full-coverage ice in a sensible way following this sort of method. One solution would be to use skin temperature, but the required multi-decadal observations are lacking. Fortunately, for the intended application here — coolling after removing the effect of anthropogenic emissions — this issue is not relevant because no regions near sea ice exhibit warming in the Nat-Hist/CMIP5-est1 attributable warming estimate.

While the results in Figure 5 look plausible, we can evaluate the method more directly by using it to estimate sea ice coverage from observed sea surface temperatures, i.e. defining the sea ice coverage:

- As full when $SST_{obs} = SST_{freeze}$ (note $SST_{obs} \geq SST_{freeze}$);
- As $m_d \cdot (SST_{obs} - SST_{open})$ when $SST_{freeze} < SST_{obs} < SST_{open}$;
- As zero when $SST_{open} < SST_{obs}$.

Results are shown in Figure 6. The estimated values tend to lag in both the spring and autumn, reflecting a lack of a consideration of freezing or melting physics in the algorithm. Coverage also tends to be underestimated during the winter by about 1 million km^2, perhaps reflecting advection of ice from frozen (at freezing-temperature) areas to nearly frozen (and above freezing) areas, a process which is not simulated by our algorithm but which is important in the Northern Hemisphere. As seen in the maps, there can be some regional differences which could be relevant for the generation of extreme weather over nearby land. However, considering the algorithm is intended only for estimating perturbations from observed conditions, this usage as a direct estimator is an extreme test; the lack of gross discrepancies is thus favourable.

5. Discussion

This paper has described the development of an estimate of the ocean warming and associated sea ice retreat attributable to anthropogenic emissions, for use in running atmospheric climate models under a scenario of what the world might have been like in the absence of emissions. Its advantages are that it uses a large amount of data from a respected source concerning the estimation of climate change (simulations submitted to the CMIP5 public data archive) and proves robust and/or stable to variations in the selection criteria of input climate model data, possible bias in the amplitude of the warming in the climate model simulations, occurrence of major volcanic eruptions, and choice of year. However, it is by no means the only possible estimate. Here we briefly mention other possible estimates related to this Nat-Hist/CMIP5-est1 estimate:

Sampling of amplitude uncertainty: The regression analysis described in Section 3.3 can also calculate the probability distribution of values for the regression coefficient informed by observed trends. Usage of the same pattern but different amplitudes corresponding to specified quantiles of this probability distribution can yield markedly different estimates of the magnitude of the role of anthropogenic emissions in the chance of extreme weather [*Pall et al.*, 2011].

Sampling individual atmosphere-ocean climate models : One possible criticism of the Nat-Hist/CMIP5-est1 estimate is that it is not necessarily physically consistent, i.e. in a nonlinear climate system averaging across models may produce changes in circulation that are not physically plausible. This issue would be remedied by selecting simulations from just a single climate model. Indeed, the few studies that have used more than one such estimate have found major differences in results, highlighting the importance of examining multiple estimates [*Pall et al.*, 2011; *Kay et al.*, 2011; *Christidis et al.*, 2012; *Shiogama et al.*, 2014; *Christidis and Stott*, 2014]. The 5-year temporal filter could be expanded to deal with the smaller sample size of simulations [*Shiogama et al.*, 2013, , Section 3.2], but not too much; spatial smoothing is another option [*Shiogama et al.*, 2013] but it would remove much of the small-scale features that are vital aspects of the differences between single-model estimates. Thus, single-model estimates would likely retain a substantial amount of sampling noise. Following the above methods (but using an 11-year temporal filter), we have thus far calculated the following single-model estimates: Nat-Hist/CanESM2-est1, Nat-Hist/CCSM4-est1 (with a 10-year filter), Nat-Hist/GISS-E2-H-p1-est1, Nat-Hist/GISS-E2-R-p1-est1, Nat-Hist/HadGEM2-ES-est1, and Nat-Hist/IPSL-CM5A-LR-est1.

Usage of a different observational data product: In the analyses shown in this paper we have used the NOAA OI.v2 product for the All-Hist ocean surface conditions as well as for developing a function for estimating the Nat-Hist/CMIP5-est1 sea ice coverage (the *Hurrell et al.* [2008] product adopts NOAA OI.v2 starting in late 1981), but removal of the anthropogenic response estimated from other observational products is also possible. The result when the HadISST1 product [*Rayner et al.*, 2003] is used for the All-Hist scenario has also been provided on the C20C+ D&A Project portal; however, because HadISST1 does not allow sea ice coverage in the 0.0–0.2 range, the NOAA OI.v2 relationship was still used for estimating the conversion function.

Usage of a different sea ice coverage estimator: Differences in treatment of how sea ice coverage should be altered may be important for attribution studies at high latitudes [*Angélil et al.*, 2014]. However, despite some effort in recent years, the *Pall et al.* [2011]

method of estimating attributable sea ice change remains the only method found to produce plausible estimates for the generic purposes considered in this paper. For instance, while *Otto et al.* [2014] used a different method following from the development of the HadISST1 product, it has substantial biases when applied to other observational products (J. Imbers, pers. comm.). A method that can yield plausible sea ice retreat would, however, be useful for examining a counterfactual world without aerosol emissions (but with historical greenhouse gas emissions), for instance.

Beyond the variations described above, other possibilities could be more observationally focussed [*Christidis and Stott*, 2014], for instance using pattern scaling methods [*Bichet et al.*, 2015]. Ultimately, it is hoped that both hardware and software will develop to the point where large-ensemble, high-spatial-resolution experiments are possible with fully coupled atmosphere-ocean-land-ice models, at which point offline estimation of the attributable ocean warming and sea ice retreat will become obsolete.

The Nat-Hist/CMIP5-est1 attributable warming estimate as well as the resultant Nat-Hist/CMIP5-est1 sea surface temperatures and sea ice concentrations when the estimate is applied to the NOAA OI.v2/*Hurrell et al.* [2008] and HadISST1 observational products are provided for use at http://portal.nersc.gov/c20c/experiment.html. Variations, following the above ideas and likely other possibilities, will also be published at this location as those estimates are developed in the near-future.

Acknowledgments. This material is based upon work supported by the U.S. Department of Energy, Office of Science, Office of Biological and Environmental Research, under contract number DE-AC02-05CH11231. This work was gratefully assisted by discussions with Myles Allen, Nikos Christidis, Jara Imbers Quintana, Cameron Rye, Hideo

Shiogama, Peter Stott, Simon Tett, and Michael Wehner, as well as the Attribution of Climate-related Events activity. The National Energy Research Scientific Computing Center's hosting of the portal from which the boundary condition fields described in this paper can be obtained is gratefully acknowledged. The authors also acknowledge the World Climate Research Programme's Working Group on Coupled Modelling, which is responsible for CMIP, and thank the climate modeling groups (listed in Table 2) for producing and making available their model output. For CMIP the U.S. Department of Energy's Program for Climate Model Diagnosis and Intercomparison provides coordinating support and led development of software infrastructure in partnership with the Global Organization for Earth System Science Portals. NOAA's Environmental Modeling Center, the Community Earth System Model project, and the U.K. Met Office are acknowledged for the NOAA OI.v2, *Hurrell et al.* [2008], and HadISST1 products respectively.

References

Allen, M. R., and P. A. Stott (2003), Estimating signal amplitudes in optical fingerprinting, part I: theory, *Clim. Dyn.*, *21*, 477–491.

Angélil, O., D. A. Stone, M. Tadross, F. Tummon, M. Wehner, and R. Knutti (2014), Attribution of extreme weather to anthropogenic greenhouse gas emissions: sensitivity to spatial and temporal scales, *Geophys. Res. Lett.*, *41*, 2150–2155, doi: 10.1002/2014GL059234.

Bichet, A., P. J. Kushner, L. Mudryk, L. Terray, and J. C. Fyfe (2015), Estimating the anthropogenic sea surface temperature response using pattern scaling, *J. Climate*, *28*, 3751–3763, doi:10.1175/JCLI-D-14-00604.1.

Bindoff, N. L., P. A. Stott, K. M. AchutaRao, M. R. Allen, N. Gillett, D. Gutzler, K. Hansingo, G. Hegerl, Y. Hu, S. Jain, I. I. Mokhov, J. Overland, J. Perlwitz, R. Sebbari, X. Zhang, and et alii (2013), Detection and attribution of climate change: from global to regional, in *Climate Change 2013: The Physical Science Basis. Contribution of Working Group I to the Fifth Assessment Report of the Intergovernmental Panel on Climate Change*, edited by T. F. Stocker, D. Qin, G.-K. Plattner, M. Tignor, S. K. Allen, J. Boschung, A. Nauels, Y. Xia, V. Bex, and P. M. Midgley, pp. 867–952, Cambridge University Press.

Christidis, N., and P. A. Stott (2014), Change in the odds of warm years and seasons due to anthropogenic influence on the climate, *J. Climate*, *27*, 2607–2621.

Christidis, N., P. A. Stott, F. W. Zwiers, H. Shiogama, and T. Nozawa (2012), The contribution of anthropogenic forcings to regional changes in temperature during the last decade, *Clim. Dyn.*, *39*, 1259–1274, doi:10.1007/s00382-011-1184-0.

Christidis, N., P. A. Stott, A. A. Scaife, A. Arribas, G. S. Jones, D. Copsey, J. R. Knight, and W. J. Tennant (2013), A new HadGEM3-A-based system for attribution of weather- and climate-related extreme events, *J. Climate*, *26*, 2756–2783.

Deser, C., A. S. Phillips, and M. A. Alexander (2010), Twentieth century tropical sea surface temperature trends revisitied, *Geophys. Res. Lett.*, *37*, L10701, doi: 10.1029/2010GL043321.

Flato, G., J. Marotzke, B. Abiodun, P. Braconnot, S. C. Chou, W. Collins, P. Cox, F. Driouech, S. Emori, V. Eyring, C. Forest, P. Gleckler, E. Guilyardi, C. Jakob, V. Kattsov, C. Reason, M. Rummukainen, and et alii (2013), Evaluation of climate models, in *Climate Change 2013: The Physical Science Basis. Contribution of Working Group I to the*

Fifth Assessment Report of the Intergovernmental Panel on Climate Change, edited by T. F. Stocker, D. Qin, G.-K. Plattner, M. Tignor, S. K. Allen, J. Boschung, A. Nauels, Y. Xia, V. Bex, and P. M. Midgley, pp. 741–866, Cambridge University Press.

Folland, C., D. Stone, C. Frederiksen, D. Karoly, and J. Kinter (2014), The International CLIVAR Climate of the 20th Century plus (C20C+) Project: Report of the Sixth Workshop, *CLIVAR Exchanges*, *19*, 57–59.

Gillett, N. P., M. F. Wehner, S. F. B. Tett, and A. J. Weaver (2004), Testing the linearity of the reponse to combined greenhouse gas and sulfate aerosol forcing, *Geophys. Res. Lett.*, *31*, L14201, doi:10.1029/2004GL020111.

Hartmann, D. L., A. M. G. Klein Tank, M. Rusticucci, L. V. Alexander, S. Brönnimann, Y. Charabi, F. J. Dentener, E. J. Dlugokencky, D. R. Easterling, A. Kaplan, B. J. Soden, P. W. Thorne, M. Wild, P. Zhai, and et alii (2013), Observations: atmosphere and surface, in *Climate Change 2013: The Physical Science Basis. Contribution of Working Group I to the Fifth Assessment Report of the Intergovernmental Panel on Climate Change*, edited by T. F. Stocker, D. Qin, G.-K. Plattner, M. Tignor, S. K. Allen, J. Boschung, A. Nauels, Y. Xia, V. Bex, and P. M. Midgley, pp. 159–254, Cambridge University Press.

Hegerl, G. C., F. W. Zwiers, P. Braconnot, N. P. Gillett, Y. Luo, J. A. Marengo Orsini, N. Nicholls, J. E. Penner, P. A. Stott, and et alii (2007), Understanding and attributing climate change, in *Climate Change 2007: The Physical Science Basis. Contribution of Working Group I to the Fourth Assessment Report of the Intergovernmental Panel on Climate Change*, edited by S. Solomon, D. Qin, M. Manning, Z. Chen, M. Marquis, K. B. Averyt, M. Tignor, and H. L. Miller, pp. 663–745, Cambridge University Press, Cambridge, U.K.

Herring, S. C., M. P. Hoerling, T. C. Peterson, and P. A. Stott (2014), Explaining extreme events of 2013 from a climate perspective, *Bull. Amer. Meteor. Soc.*, *95*, S1–S96.

Hoegh-Guldberg, O., R. Cai, E. s. Poloczanska, P. G. Brewer, S. Sundby, K. Hilmi, V. J. Fabry, S. Jung, and et alii (2014), The ocean, in *Climate Change 2014: Impacts, Adaptation, and Vulnerability. Part B: Regional Aspects. Contribution of Working Group II to the Fifth Assessment Report of the Intergovernmental Panel on Climate Change*, edited by V. R. Barros, C. B. Field, and et alii, pp. 1655–1731, Cambridge University Press.

Hurrell, J. W., J. J. Hack, D. Shea, J. M. Caron, and J. Rosinski (2008), A new sea surface temperature and sea ice boundary dataset for the Community Atmosphere Model, *J. Climate*, *21*, 5145–5153.

Karl, T. R., A. Arguez, B. Huang, J. H. Lawrimore, J. R. McMahon, M. J. Menne, T. C. Peterson, R. S. Vose, and H.-M. Zhang (2015), Possible artifacts of data biases in the recent global surface warming hiatus, *Science*, *348*, 1469–1472, doi: 10.1126/science.aaa5632.

Kay, A. L., S. M. Crooks, P. Pall, and D. A. Stone (2011), Attribution of Autumn/Winter 2000 flood risk in England to anthropogenic climate change: a catchment-based study, *J. Hydrol.*, *406*, 97–112, doi:10.1016/j.jhydrol.2011.06.006.

Kennedy, J. J. (2014), A review of uncertainty in in situ measurements and data sets of sea surface temperature, *Rev. Geophys.*, *52*, 1–32, doi:10.1002/2013RG000434.

Mahlstein, I., P. R. Gent, and S. Solomon (2013), Historical Antarctic mean sea ice area, sea ice trends, and winds in CMIP5 simulations, *J. Geophys. Res.*, *118*, 5105–5110, 10.1002/jgrd.50443.

Meehl, G. A., W. M. Washington, T. M. L. Wigley, J. M. Arblaster, and A. Dai (2003), Solar and greenhouse gas forcing and climate response in the twentieth century, *J. Climate*, *16*, 426–444.

Notz, D. (2014), Sea-ice extent and its trend provide limited metrics of model performance, *Cryosphere*, *8*, 229–243, doi:10.5194/tc-8-229-2014.

Otto, F. E. L., S. M. Rosier, M. R. Allen, N. R. Massey, C. J. Rye, and J. Imbers Quintana (2014), Attribution analysis of high precipitation event in summer in England and Wales over the last decade, *Clim. Change*, doi:10.1007/s10584-014-1095-2.

Pall, P., T. Aina, D. A. Stone, P. A. Stott, T. Nozawa, A. G. J. Hilberts, D. Lohmann, and M. R. Allen (2011), Anthropogenic greenhouse gas contribution to flood risk in England and Wales in Autumn 2000, *Nature*, *470*, 382–385.

Rayner, N. A., D. E. Parker, E. B. Horton, C. K. Folland, L. V. Alexander, D. P. Rowell, E. C. Kent, and A. Kaplan (2003), Global analyses of sea surface temperature, sea ice, and night marine air temperature since the late nineteenth century, *J. Geophys. Res.*, *108*, 4407, doi:10.1029/2002JD002670.

Reynolds, R. W., N. A. Rayner, T. M. Smith, D. C. Stokes, and W. C. Wang (2002), An improved in situ and satellite SST analysis for climate, *J. Clim.*, *15*, 1609–1625.

Ribes, A., and L. Terray (2013), Application of regularised optimal fingerprinting to attribution. Part II: application to global near-surface temperature, *Clim. Dyn.*, *41*, 2837–2853, doi:10.1007/s00382-013-1736-6.

Shiogama, H., D. A. Stone, T. Nagashima, T. Nozawa, and S. Emori (2012), On the linear additivity of climate forcing-response relationships at global and continental scales, *International Journal of Climatology*, *33*, 2542–2550.

Shiogama, H., M. Watanabe, Y. Imada, M. Mori, M. Ishii, and M. Kimoto (2013), An event attribution of the 2010 drought in the South Amazon region using the MIROC5 model, *Atmos. Sci. Lett.*, *14*, 170–175.

Shiogama, H., M. Watanabe, Y. Imada, M. Mori, Y. Kamae, M. Ishii, and M. Kimoto (2014), Attribution of the June-July 2013 heat wave in the southwestern United States, *SOLA*, *10*, 122–126, doi:10.2151/sola.2014-025.

Stott, P. A., M. R. Allen, N. Christidis, R. Dole, M. Hoerling, C. Huntingford, P. Pall, J. Perlwitz, and D. A. Stone (2013), Attribution of weather and climate-related extreme events, in *Climate Science for Serving Society: Research, Modelling and Prediction Priorities*, edited by G. R. Asrar and J. W. Hurrell, pp. 307–337, Springer.

Taylor, K. E., R. J. Stouffer, and G. A. Meehl (2012), An overview of CMIP5 and the experiment design, *Bull. Amer. Met. Soc.*, *93*, 485–498.

Trenberth, K. E., J. T. Fasullo, and T. G. Shepherd (2015), Attribution of climate extreme events, *Nature Clim. Change*, doi:10.1038/NCLIMATE2657.

Wolski, P., D. Stone, M. Tadross, M. Wehner, and B. Hewitson (2014), Attribution of floods in the Okavango Basin, Southern Africa, *J. Hydrol.*, *511*, 350–358.

Table 1. List of time-varying boundary conditions for use in the All-Hist/est1 experiment and the various experiments in the Nat-Hist family.

Forcing	**All-Hist/est1**	**Nat-Hist family**
Greenhouse gas concentrations	Historical values	Pre-industrial values
Anthropogenic aerosol burdens or emissions	Historical values	Pre-industrial values
Stratospheric ozone	Historical values	Pre-industrial values
Land cover	Historical values	Historical values
Solar luminosity	Historical values	Historical values
Natural aerosol burdens or emissions	Historical values	Historical values
Sea surface temperatures	Historical values	Modified historical values
Sea ice concentrations	Historical values	Modified historical values

Table 2. List of CMIP5 simulations of atmosphere-ocean models used for estimating the adjustment of the sea surface temperatures for the Nat-Hist/CMIP5-est1 scenario. Simulation labels apply to each of the "historical", "rcp45", and "historicalNat" scenarios. rcp45 simulations continue from historical simulations with the handover on 1 January 2006, while historicalNat simulations end in different years, depending on the model. A total of 51 simulations from 19 CMIP5 models for each of the scenarios are included in the calculation. Simulation labels apply across all scenarios.

CMIP5 Model	**Simulation labels**	**Last year of HistoricalNat simulations**
BCC-CSM1-1	r1i1p1	2012
BNU-ESM	r1i1p1	2005
CanESM2	r1i1p1, r2i1p1, r3i1p1, r4i1p1, r5i1p1	2012
CCSM4	r1i1p1, r2i1p1, r4i1p1, r6i1p1	2005
CNRM-CM5	r1i1p1	2012
CSIRO-Mk3-6-0	r1i1p1, r2i1p1, r3i1p1, r4i1p1, r5i1p1	2012
GFDL-CM3	r1i1p1	2005
GFDL-ESM2M	r1i1p1	2005
GISS-E2-H-p1	r1i1p1, r2i1p1, r3i1p1, r4i1p1, r5i1p1	2012
GISS-E2-H-p3	r1i1p3, r2i1p3, r3i1p3, r4i1p3, r5i1p3	2012
GISS-E2-R-p1	r1i1p1, r2i1p1, r3i1p1, r4i1p1, r5i1p1	2012
GISS-E2-R-p3	r1i1p3, r2i1p3, r3i1p3, r4i1p3, r5i1p3	2012
HadGEM2-ES	r1i1p1, r2i1p1, r3i1p1, r4i1p1	2018/2019
IPSL-CM5A-LR	r1i1p1, r2i1p1, r3i1p1	2012
IPSL-CM5A-MR	r1i1p1	2012
MIROC-ESM	r1i1p1	2005
MIROC-ESM-CHEM	r1i1p1	2005
MRI-CGCM3	r1i1p1	2005
NorESM1-M	r1i1p1	2012

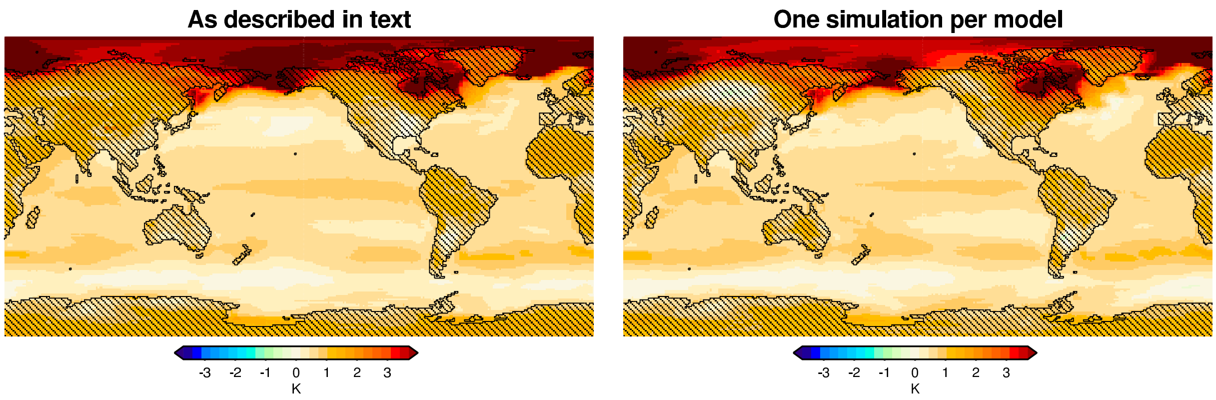

Figure 1. Estimates of attributable ocean warming for January 2001 using all selected CMIP5 simulations (left) or only one simulation (per scenario) per climate model (right). A 5-year temporal filter was used in all calculations.

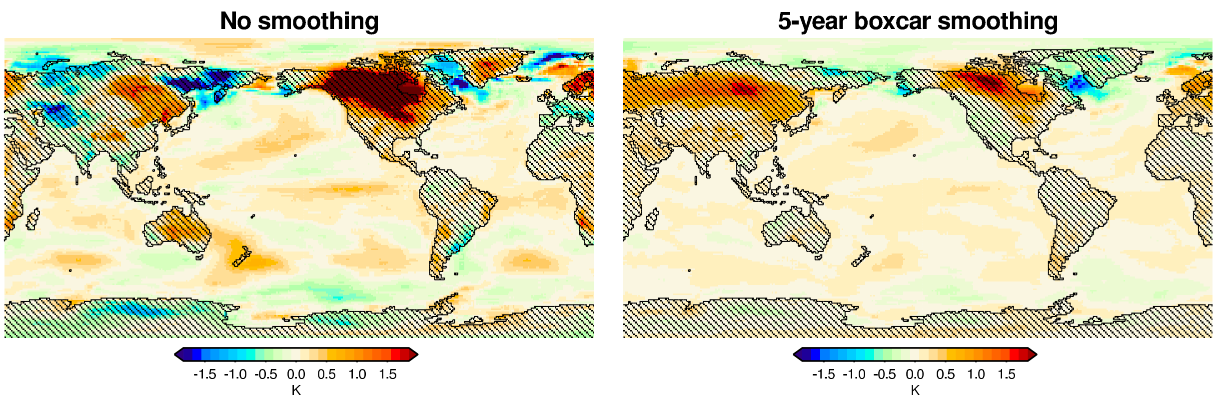

Figure 2. Maps of the difference in estimated attributable warming for January 2006 versus January 2001. The left map is produced without temporal smoothing, while the right map uses a 5-year boxcar filter applied to January data.

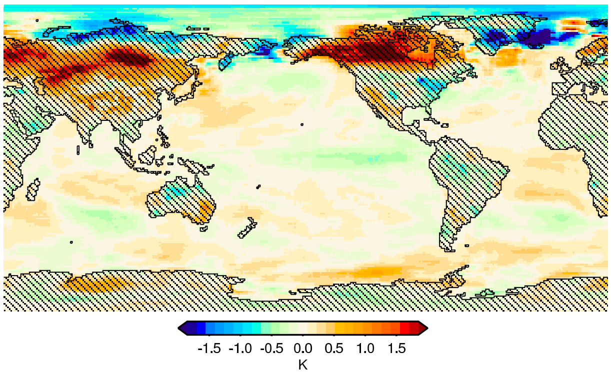

Figure 3. Map of the difference in estimated attributable warming for January 1997 versus January 1992. No temporal filter applied in the calculation.

Table 3. 90% confidence ranges on regression coefficients from comparison of the observed sea surface temperature record against the Nat-Hist/CMIP5-est1 climate model output. The confidence ranges and goodness-of-fit are estimated with unforced simulations providing 79 samples for 110-year trends and 175 for 50-year trends. Values marked with asterisks fail the goodness-of-fit test.

Period	**Domain**	**Annual**	**January**	**April**	**July**	**October**
1901–2010	Ocean, global	0.87,1.16*	0.83,1.12*	0.87,1.18*	0.88,1.19*	0.87,1.15*
1901–2010	Ocean, 50°S–50°N	0.91,1.19*	0.87,1.16*	0.90,1.20*	0.91,1.20*	0.91,1.18*
1961–2010	Ocean, global	0.58,1.02	0.47,0.96	0.62,1.08	0.64,1.09	0.55,0.99
1961–2010	Ocean, 50°S–50°N	0.62,1.05	0.54,0.99	0.65,1.09	0.65,1.09	0.60,1.03

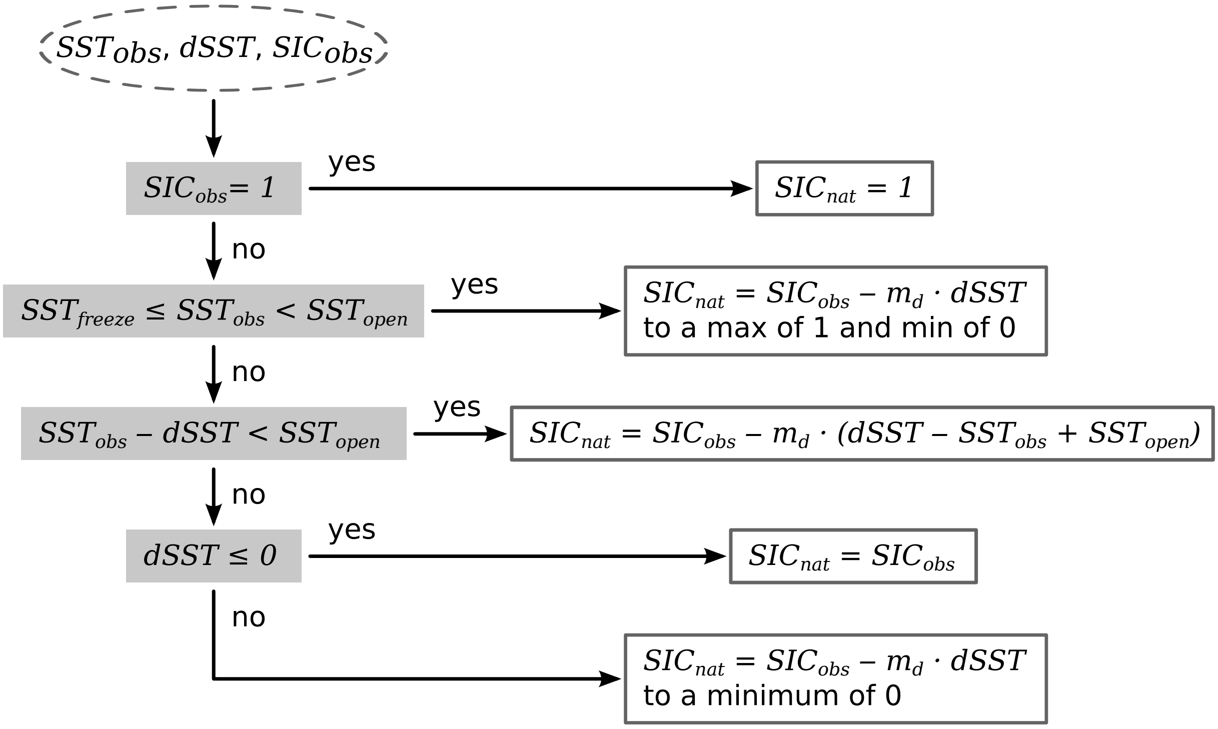

Figure 4. The algorithm used for estimating Nat-Hist fractional sea ice coverage, SIC_{nat}, in a cell on the target spatial grid. The inputs are the observed (also used as All-Hist) sea surface temperature, SST_{obs}, and fractional sea ice coverage, SIC_{obs}, along with the attributable warming estimate for the location, $dSST$. Note that in the case of warming attributable to anthropogenic emissions, we expect $dSST > 0$. SST_{freeze} is the freezing temperature of sea water (-1.8°C in the NOAA OI.v2 observationally-based data product). See text for further details.

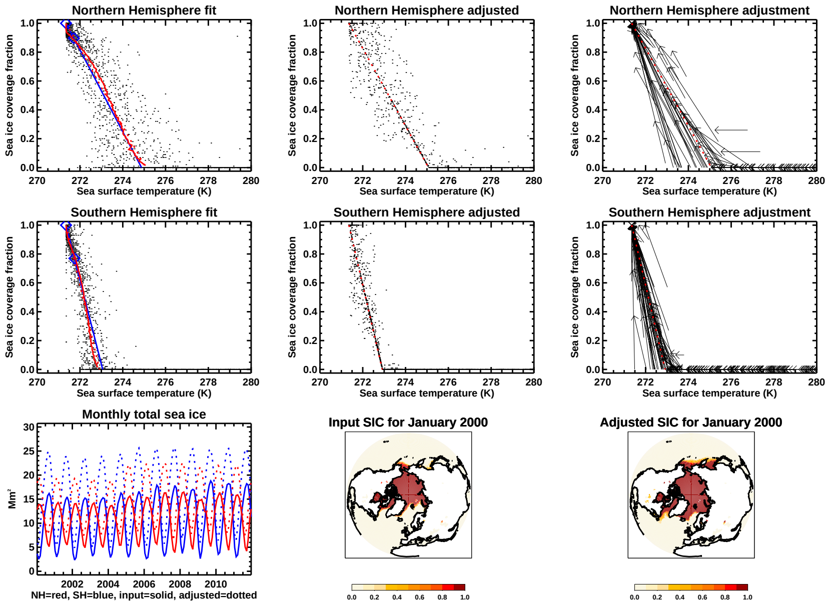

Figure 5. The estimation of attributable changes in sea ice coverage as implemented for the Nat-Hist/CMIP5-est1 scenario. The top two rows show data for the Northern Hemisphere (top row) and Southern Hemisphere (middle row). The left panels of these two rows show the sea ice coverage and sea surface temperature relationship during the 2001-2010 period in the NOAA OI.v2 observational product [*Reynolds et al.*, 2002] (dots), the *Pall et al.* [2011] linear fit for adjusting ice coverage (blue line, with the diamonds marking the points used to calculate the line), and the median temperature for each coverage bin (solid red line) and the resulting linear fit (dashed red line) used for the Nat-Hist/CMIP5-est1 scenario. (Only a limited number of points are displayed in order to avoid saturation.) The middle panels in the top two rows show the resulting temperature and coverage data estimates for the Nat-Hist/CMIP5-est1 scenario, while the right panels show the progression from observed values to Nat-Hist/CMIP5-est1 values. The bottom left panel shows the monthly coverage time series for both hemispheres (North in red, South in blue) as observed (solid) and under the Nat-Hist/CMIP5-est1, based on NOAA OI.v2. The two maps illustrate Arctic coverage for January 2000 from observations (middle) and for the Nat-Hist/CMIP5-est1 scenario (right).

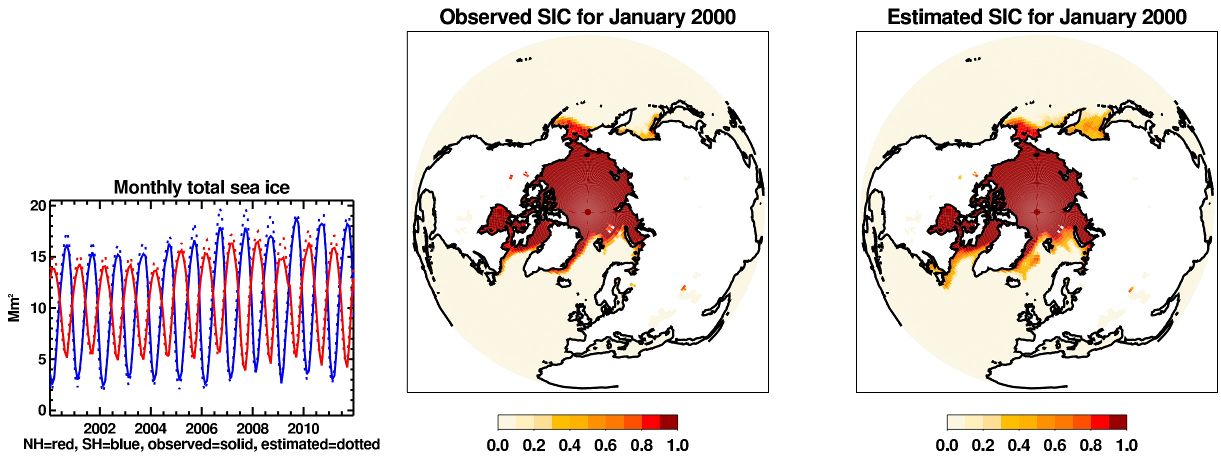

Figure 6. Comparison of sea ice coverage calculated directly using the algorithm developed here versus observed values. Left panel: Monthly mean values for the Northern (red) and Southern (blue) Hemispheres from the NOAA OI.v2 observational product (solid) and as estimated from the NOAA OI.v2 sea surface temperatures (dotted). Middle panel: Observed sea ice concentration according to NOAA OI.v2 for January 2000. Right panel: Estimated sea ice concentration based on NOAA OI.v2 sea surface temperatures.